

Optimal strategies for adaptive cruise control

Original

Optimal strategies for adaptive cruise control / Mba, CLEMENT UCHECHUKWU; Novara, Carlo - In: Communications in Computer and Information Science[s.l.] : Springer Verlag, 2017. - ISBN 9783319637112. - pp. 227-241 [10.1007/978-3-319-63712-9_13]

Availability:

This version is available at: 11583/2678902 since: 2020-06-04T10:18:10Z

Publisher:

Springer Verlag

Published

DOI:10.1007/978-3-319-63712-9_13

Terms of use:

This article is made available under terms and conditions as specified in the corresponding bibliographic description in the repository

Publisher copyright

Springer postprint/Author's Accepted Manuscript

This version of the article has been accepted for publication, after peer review (when applicable) and is subject to Springer Nature's AM terms of use, but is not the Version of Record and does not reflect post-acceptance improvements, or any corrections. The Version of Record is available online at: http://dx.doi.org/10.1007/978-3-319-63712-9_13

(Article begins on next page)

Optimal strategies for adaptive cruise control

Clement U. Mba and Carlo Novara

Department of Mechanical and Aerospace Engineering

Department of Control and Computer Engineering

Politecnico di Torino, Corso Duca degli Abruzzi, 24, Torino, Italy

`{clement.mba,carlo.novara}@polito.com`

Abstract. In addition to providing good tracking capability and reducing fuel consumption, an Adaptive Cruise Control (ACC) system is required to be very comfortable. Although several appealing ACC policies have been introduced so far, a few of which are currently in use, it is still difficult in general to find an ACC policy that is able to optimally combine requirements such as high safety, low fuel consumption and satisfactory comfort level. Additionally, no systematic methods are available for the optimization of a control policy performance. This chapter addresses these problems by comparing different ACC policies and developing an optimization method based on a multi-objective Pareto criterion, finalized at designing policies with an all around performance. Furthermore, the designed optimal policy is tested in view of its application on real vehicles via simulations.

Keywords: Adaptive Cruise Control, test simulation, performance optimization.

1 Introduction

Driving can be defined as a set of operations aimed at controlling a motor vehicle, where control is typically performed by a human driver. However, the human driver behavior may tend sometimes to cause undesirable vehicle behaviors. In modern vehicles, to avoid or prevent these kinds of behaviors, control is usually

done by the human driver with the help of some Driver Assistance Systems, one of the most important of which is the Cruise Control.

Cruise Control (CC) has the task of maintaining the vehicle speed at a desired value. However, a drawback of CC is that it cannot vary the speed of the vehicle: whenever a vehicle in front of the vehicle equipped with CC is traveling slower than the latter, the driver has to step on the brakes in order to deactivate the Cruise Control and step on the accelerator when the preceding vehicle speeds up [2]. As a result, Cruise Control has to be reset from time to time. This drawback is overcome by the more advanced Adaptive Cruise Control (ACC), which is able to adjust the speed of the vehicle, depending on various factors influencing it without manual intervention from the driver [2],[3],[4]. Some of them, like the “stop and go”, can bring the vehicle to a stop and start it moving [3],[4].

In general, the design of an ACC begins with an ACC policy. Different ACC policies have been proposed: Constant Time Gap (CTG), Constant Distance, Constant acceptance, Constant Stability and Constant safety factor [1]. ACC policies specify the desired steady state distance between two vehicles in succession. Note that ACC policies can be either autonomous [5], cooperative [6],[7] or a combination of both [8]. Introducing and maintaining continuous inter-vehicular communication, which is the main feature of cooperative policies causes network effects that can undermine the performance of the ACC [7]. Moreover, maintaining continuous inter-vehicular communication is costly [9],[11]. Thus, the autonomous operation seems like the most preferred choice at present, and it is the area of focus in this paper.

The performance of an ACC system is based on the particular control policy that it employs. The basic control policies are the Constant Spacing Policy (CSP), Constant Time Gap (CTG) and Variable Time Gap (VTG). All the other policies are usually variants of these basic policies. However, even though all these policies are appealing from a methodological point of view, it is difficult in general to understand which is the actual performance that can be guaranteed on a real vehicle. Another relevant issue is that, to the best of our knowledge,

no systematic methods can be found for the optimization of the control policy performance.

In this perspective, the main contributions of the paper are two. First, the control policies employed by the “standard” ACC systems are compared by means of extensive simulations, considering different realistic road scenarios. This kind of study is important to understand which control policies and, more in general, which control approaches can be more effective in view of their implementation on real vehicles. Second, an optimization strategy based on a multi-objective Pareto criterion is proposed, finalized at designing high-performance control policies. The strategy is tested by means of extensive simulations, involving different realistic road scenarios. These simulations show that the method allows the design of control policies able to perform significantly better with respect to the “standard” policies, in terms of safety, fuel consumption and comfort.

2 Vehicle model and control policies

In this section, we introduce the vehicle and control models that will be used in the simulations, first to compare the “standard” ACC systems, then to test our optimal control policy design method.

The following assumptions were made:

- All vehicles are identical and move in a straight line.
- Before the maneuver of the lead vehicle, all the vehicles were moving at the same steady state speed.
- The lead vehicle takes a finite amount of time to perform a maneuver prior to reaching steady state speed.

The longitudinal dynamics of each vehicle (plant) can be approximated by the following model (see [5],[12],[13]):

$$\tau \ddot{p} + \dot{p} = u \quad (1)$$

where p is the vehicle longitudinal position, u represents a “desired” longitudinal acceleration and τ is the vehicle time constant.

The desired acceleration u is the control input, which can be used to improve the vehicle performance in terms of safety, comfort and fuel consumption. This task can be accomplished by a proper control policy, as shown schematically in Fig. 1, where the block “Vehicle” is a dynamic system described by (1) and ϵ is the spacing error to be defined subsequently.

Usually, the control policies should satisfy string stability requirements in order to give a good performance. String stability is defined as stability with respect to the spacing between vehicles. It ensures that the spacing error, defined as the difference between the actual and desired spacing, do not get larger as it propagates upstream in a string of Adaptive Cruise Control vehicles using the same control law [5],[8],[11],[12],[13],[14]. The CSP policy requires inter-vehicular communication if string stability is to be guaranteed [11],[15], while the CTG and VTG policies overcome this limitation [9],[11],[13]. Since we are only considering the autonomous operation, our tests are conducted only on the CTG and VTG policies.

The CTG policy is defined by the control law

$$\begin{aligned} u &= -\frac{(\dot{p} - \dot{p}_f + \lambda\epsilon)}{h} \\ \epsilon &= p - p_f + L_{des} \end{aligned} \tag{2}$$

where p and p_f are the positions of a vehicle and the preceding vehicle respectively, and ϵ is the deviation from the desired spacing, otherwise known as the spacing error, [5],[12],[13],[17].

λ , L_{des} and h are design parameters, to be chosen in order to obtain the desired longitudinal dynamics performance. λ is a control gain, L_{des} is the desired spacing between the vehicles and h is called the time gap (it represents the time distance between the two vehicles).

Combining the vehicle equation (1) with the control equations (2), we obtain an Linear Time Invariant (LTI) system, with input p_f and output $y = \epsilon$. Note

that, on a vehicle equipped with an ACC systems, p_f is typically measured by a radar.

The VTG has several variants [9],[12],[16],[17],[18],[19],[20], which are similar to each other. The Nonlinear Range Policy (NRP) [16, 20] is considered here because of its simple structure. This policy is defined by the control law

$$u = (1 - \frac{\tau k}{h} - \frac{\tau \lambda k}{h^2} \frac{h^2}{k}) \ddot{p} + (\frac{\tau k}{h^2}) \dot{p}_f - \dot{p} \quad (3)$$

where k is a design parameter, called the scaling factor [16],[20].

As for the VTG policy, combining the vehicle equation (1) with the control equations (3), we obtain an LTI system, with input p_f and output $y = \varepsilon$.

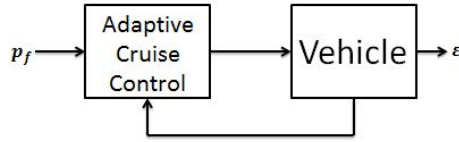


Fig. 1. Adaptive Cruise Control structure.

3 ACC policies comparison

The two ACC policies described in Section 2 are tested considering three different scenarios:

Scenario 1. Constant number of vehicles traveling in a line

In this scenario, 10 vehicles are traveling in a line and the lead vehicle makes some critical manoeuvre. Three kinds of critical manoeuvres are simulated -
 Manoeuvre 1: The lead vehicle suddenly increases its speed; this manoeuvre was obtained simulating u_1 (the input of the leading vehicle) as a filtered positive step.
 Manoeuvre 2: The lead vehicle suddenly increases its speed and then goes back to the original speed; this manoeuvre was obtained simulating u_1 as a filtered positive impulse.
 Manoeuvre 3: The lead vehicle decelerates continuously; this manoeuvre was obtained simulating u_1 as a filtered negative ramp.

Scenario 2. Vehicles joining and leaving the line

In this scenario, 10 vehicles are traveling in a line and one or more vehicles join or leave the line at different times; this manoeuvre was simulated just by suddenly increasing or decreasing the number of vehicles in the line with the gap between the vehicles taken into consideration to prevent collision. Note that this simulation is more challenging than a real situation, where the process of joining or leaving the line is “more continuous”. We considered up to 5 vehicles joining or leaving the line.

Scenario 3. Traffic flow

In this scenario, 10 vehicles are traveling in a line and one or more vehicles join or leave the line at different times. We considered up to 5 vehicles joining or leaving the line. As an additional complication, the line may stop at different times due to the presence of traffic lights; The stop at the light was obtained simulating u_1 as a filtered negative ramp that, after a certain time, becomes constant.

We considered different combinations of the values of the parameters characterising the vehicle model and the control policies. In particular, the following parameter ranges were assumed:

$$\tau \in [0.5, 0.95] \text{ s}$$

$$\lambda \in [0.4, 2]$$

$$h \in [0.1, 2] \text{ s}$$

$$k \in [2, 15]$$

$$L_{des} = 40 \text{ m}.$$

For each manoeuvre of scenario 1 and for each parameter combination, we performed one simulation. This simulation was long enough to reach steady-state conditions. For each of scenarios 2 and 3 and for each parameter combination, we performed a sufficiently long simulation, in order to capture all relevant situations that can occur in a real road scenario. In particular, the duration of the simulated road scenarios was about 107 hours, corresponding to about 4 hours

of Matlab run time. The simulations were done using Matlab R2014a and its simulink environment.

To evaluate the performance of an ACC control policy, we considered the following indexes:

- *Recovery time*: The recovery time of a vehicle is defined

$$T_R = T_{ss} - T_c$$

where T_c is the time at which a critical event occurs (e.g., a critical manoeuvre, a vehicle joining or leaving the line, or a stop at the light) and T_{ss} is the 2% settling time (that is, the time after which the system output is always within an interval with center at the steady-state value of the output and amplitude 2% of this value).

- *Input signal Root Mean Square value*:

$$RMS_u = \|\tilde{u}\|_2 / \sqrt{N} \quad (4)$$

where \tilde{u} is the (discrete-time) command input signal of a vehicle acquired from the simulation, $\|\cdot\|_2$ is the vector 2-norm and N is the length of \tilde{u} .

- *Output signal Root Mean Square value*:

$$RMS_y = \|\tilde{y}\|_2 / \sqrt{N} \quad (5)$$

where \tilde{y} is the acquired (discrete-time) output signal of a vehicle.

- *Peak input signal*:

$$MAX_u = \|\tilde{u}\|_\infty \quad (6)$$

where $\|\cdot\|_\infty$ is the vector ∞ -norm.

- *Peak output signal*:

$$MAX_y = \|\tilde{y}\|_\infty. \quad (7)$$

The recovery time measures the capability of the control policy to promptly bring the vehicle back to its “normal” operation conditions. RMS_y and MAX_y essentially measures the mean deviation of the output from the desired value (hence, it is also an indirect measure of the recovery time). RMS_u and MAX_u

are related to the energy spent by the control policy in order to obtain the desired performance while RMS_J is related to passenger comfort in a vehicle.

Table 1. Scenario 1, Manoeuvre 1. Average performance indexes

Strategy	\bar{T}_R [s]	\bar{RMS}_u	\bar{RMS}_y
CTG	33.14	12.508	1.1199
NRP	4.5	14.7154	0.1833

Table 2. Scenario 1, Manoeuvre 2. Average performance indexes

Strategy	\bar{T}_R [s]	\bar{RMS}_u	\bar{RMS}_y
CTG	36.7	0.0228	0.0286
NRP	5.14	0.0820	0.0237

Table 3. Scenario 1, Manoeuvre 3. Average performance indexes

Strategy	\bar{T}_R [s]	\bar{RMS}_u	\bar{RMS}_y
CTG	6.7	35.3265	1.5331
NRP	0.55	45.1805	0.0996

Tables 1-6 show the performance indexes obtained in the simulations, averaged over all the vehicles composing the line, all the critical events (i.e., vehicles joining and leaving the line and stops at the lights) and all the parameter combinations. The averages are indicated with a bar. In Figures 2-6, we can observe the performance indexes obtained in the simulations, averaged over all the vehicles composing the line and all the critical events.

Tables 1, 2 and 3 show that the NRP generally recovers faster when subjected to critical conditions, involving also lower values of \bar{RMS}_y . However, the required

Table 4. Scenario 2, Vehicles joining. Average performance indexes

Strategy	$R\bar{M}S_u$	$R\bar{M}S_y$
CTG	111.7	6.9109
NRP	115.3	5.8677

Table 5. Scenario 2, Vehicles leaving. Average performance indexes

Strategy	$R\bar{M}S_u$	$R\bar{M}S_y$
CTG	109.6	7.1459
NRP	114	6.0608

command activity, measured by $R\bar{M}S_u$, is higher. Similar results are shown by Tables 4, 5 and 6.

Given that $\tau \geq 0.5$ and $\lambda = 0.4$, the NRP is more flexible than the CTG, in the sense that h can be varied from 0.1 to more than 1.8 without the spacing errors getting larger as they propagate upstream in vehicles using NRP. When $h = 0.1$, for the NRP the recovery time as well as the $R\bar{M}S_y$ value is “small”, with a high value of $R\bar{M}S_u$ on the command input activity.

The average recovery time increases a little for vehicles using the NRP as τ gets higher. In the case of the CTG, the average recovery time increases considerably as τ gets higher. Accordingly, it can be said that higher values of τ for each of the vehicles do not have as much influence on vehicles using the NRP as they do on vehicles that use the CTG. This is most likely to be a result of the high value of h that is required in the CTG when $\tau > 0.5$, to prevent the spacing errors from getting larger as they propagate upstream.

Table 6. Scenario 3. Average performance indexes

Strategy	$R\bar{M}S_u$	$R\bar{M}S_y$
CTG	436	5.608
NRP	441.7	4.191

The simulation results obtained from scenario 2, as shown in Figures 2 and 3, and scenario 3, as shown in Figures 4 and 5, show that the NRP has lower $R\bar{M}S_y$ than the CTG for the same values of h and τ . The two lines with the same h in Figures 2 and 3 correspond to the vehicles either joining or leaving the line. It should also be noted that similar results are obtained when τ is different for each vehicle in the stream.

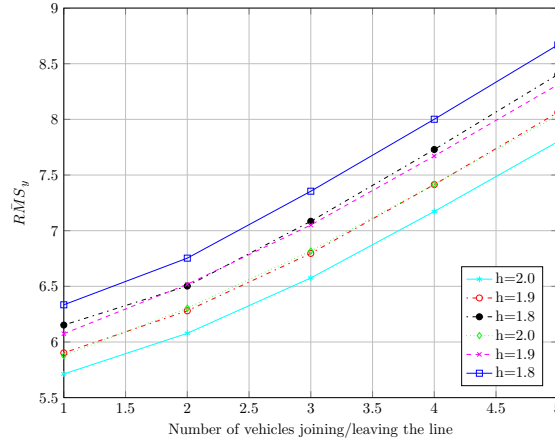


Fig. 2. Scenario 2 (CTG with $\tau = 0.5s$, $\lambda = 0.4$)

Low values of the time gap as well as low values of $R\bar{M}S_u$ are desirable but these act in contrast to each other. As stated earlier, lower values of the time gap require higher command input activity. Indeed, $R\bar{M}S_u$ and $R\bar{M}S_y$ are two contrasting criteria. This is important for the NRP, since it can sustain $h \in [0.1, 2]$. It is our deduction that if h remains in a “low value zone” for instance $h \in [0.1, 0.3]$ for a long time during driving, a lot of energy due to control activity might be expended. A possible way to mitigate this could be to design the control algorithm in such a way that the time gap does not exceed a certain amount of time when it is in the “low value zone”. It is important to determine the right amount of time. This amount of time could depend on whether there are vehicles joining or leaving the stream as well as on their

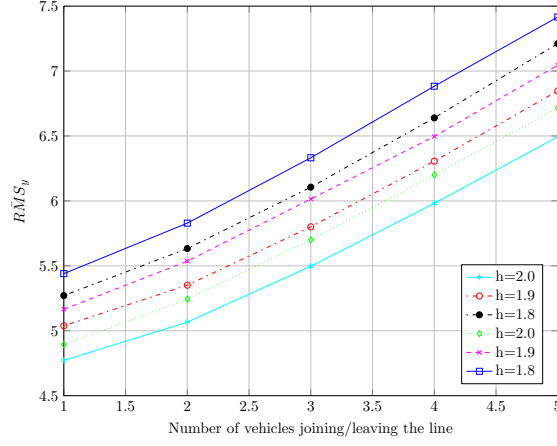


Fig. 3. Scenario 2 (NRP with $\tau = 0.5s$, $\lambda = 0.4$, $k = 4$)

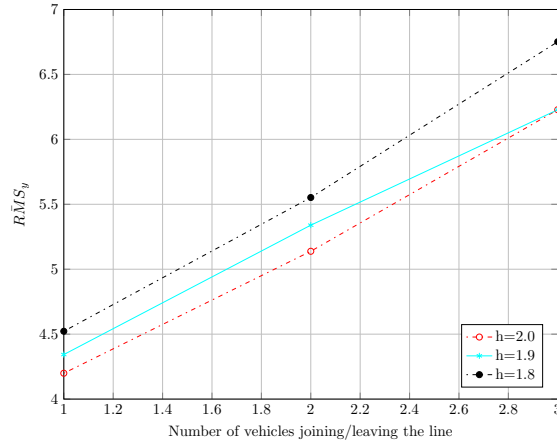


Fig. 4. Scenario 3 (CTG with $\tau = 0.5$, $\lambda = 0.4$)

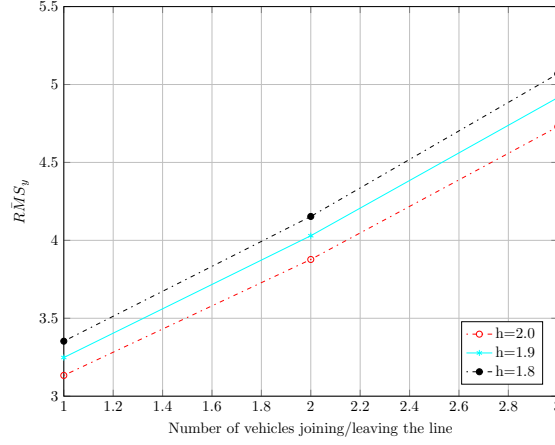


Fig. 5. Scenario 3 (NRP with $\tau = 0.5$, $\lambda = 0.4$, $k = 4$)

number, or on what the design objective of the car manufacturer is (i.e, energy reduction or inter-vehicular space reduction to increase traffic output).

4 Optimization Strategy

As discussed in the previous section, in the design of an ACC system there is a trade-off between two contrasting requirements. On the one hand, the ACC system must provide a satisfactory performance in terms of safety and prompt answer to external disturbances. On the other hand, the ACC system must not require a too large command activity, which may lead to a high consumption of fuel and/or electrical power.

To quantify the ACC performance we hereby consider the RMS_y index defined in (5). To quantify the command activity we consider the RMS_u index defined in (4). We would like to minimise both these coefficients but clearly this cannot be done, since these indexes are in contrast with each other. In other words, we are dealing with a multi-objective optimization problem.

This kind of problems can be efficiently solved considering a Pareto optimality criterion, [21]. Let $RMS_y(C)$ and $RMS_u(C)$ be respectively the performance and

command activity indexes of a given ACC controller C . A controller C^1 is said to *dominate* another controller C^2 if

$$\begin{aligned} & RMS_y(C^1) \leq RMS_y(C^2) \text{ and } RMS_u(C^1) < RMS_u(C^2) \\ & \text{or} \\ & RMS_y(C^1) < RMS_y(C^2) \text{ and } RMS_u(C^1) \leq RMS_u(C^2). \end{aligned} \tag{8}$$

A controller C^* is said *Pareto optimal* if it is not dominated by any other one. In other words, no other controller exists that can be overall better than an optimal controller. If a controller is better than an optimal one with regard to a single objective (e.g., $RMS_u(C)$), it is certainly worse with respect to the other (e.g., $RMS_y(C)$). The set of Pareto optimal controllers define a curve in the performance index space called *Pareto front* (see the green line in Fig. 6).

Based on these concepts, the optimization strategy that we propose is as follows:

- Perform a Monte Carlo simulation, consisting of N_T trials.
- In each trial:
 - Choose random values of the parameters h , k and λ (clearly, these values must be reasonable from a physical point of view). Each parameter 3-tuple defines a controller C^i , with $i = 1, \dots, N_T$.
 - For the chosen parameter 3-tuple, perform N_S simulations considering realistic road scenarios.
 - compute the averages $\bar{RMS}(C^i)_y$ and $\bar{RMS}(C^i)_u$ of the N_S values of $RMS(C^i)_y$ and $RMS(C^i)_u$.
- Considering that the pairs $(\bar{RMS}(C^i)_y, \bar{RMS}(C^i)_u)$, with $i = 1, \dots, N_T$, define points in the two-dimensional performance index space, construct the Pareto optimality front, using (8) to individuate those controllers that are not dominated.

Note that τ and L_{des} are assumed fixed but they can be included in the optimization process without significant modifications.

Following this strategy, a Monte Carlo simulation was performed, with $N_T = 4760$. In each trial, random values of h , k and λ were taken from the intervals $[0.1, 2]$, $[2, 15]$ and $[0.4, 2]$, respectively (a uniform distribution was considered for all the three parameters). The values $\tau = 0.5$ s and $L_{des} = 40$ m were also assumed. For each random 3-tuple (corresponding to a randomly generated controller), $N_S = 10$ simulations were performed considering Scenario 3 (traffic flow with 10 vehicles in a line and 5 vehicles randomly joining or leaving the line). Then, the performance averages $R\bar{M}S(C^i)_y$ and $R\bar{M}S(C^i)_u$ were computed. Finally, the Pareto optimality front was constructed.

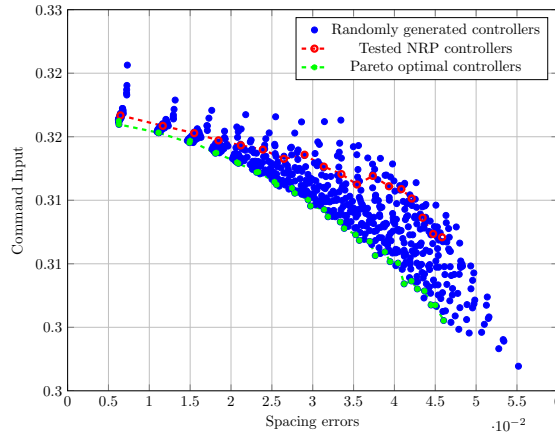


Fig. 6. Pareto optimization

The results of this procedure are shown in Fig. 6. We can distinguish a number of randomly generated controllers (blue dots) and the Pareto optimal controllers (green line). These are compared with the tested NRP controllers (red dots). The performance in terms of spacing errors of a set of “standard” vehicles and a set of Pareto optimal vehicles is plotted in Figures 7 and 8, respectively. These results show that an improvement of about 30% can be obtained using a Pareto optimal controller with respect to using a “standard” controller, indicating that the proposed optimization strategy can lead to high-performance ACC systems.

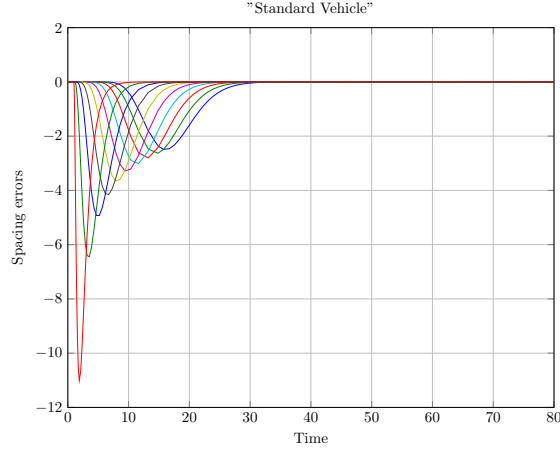


Fig. 7. Performance of the NRP controllers ($\tau = 0.5s$, $L_{des} = 40m$, $h = 1.3s$, $k = 4$, $\lambda = 0.4$). The different lines correspond to the spacing errors of each NRP controlled vehicle in the stream.

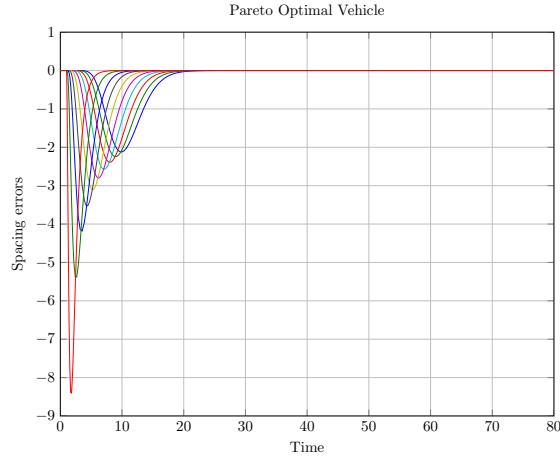


Fig. 8. Performance of the Pareto optimal controllers ($\tau = 0.5s$, $L_{des} = 40m$, $h = 0.9s$, $k = 10$, $\lambda = 1.6$). The different lines correspond to the spacing errors of each Pareto optimal vehicle in the stream.

5 Comfort analysis

While reduced spacing errors and command inputs can help to improve the safety and to lower the fuel consumption, the aspect of comfort is also very important. Indeed, comfort is commonly considered a very important and vital part of vehicle design and ergonomics. According to some studies, comfort is a crucial requirement that passengers consider when evaluating a vehicle. Most passengers cite discomfort as the reason for not using ACC [22]. Thus, ACCs with a suitable amount of comfort could lead to a higher acceptance of ACCs by the society.

Generally, the comfort of passengers in ground transport systems is deduced from motion changes in all directions and other environmental issues [23]. An efficient and simple way of estimating the comfort level of a vehicle is to calculate the rate of change of acceleration of the vehicle, that is, the jerk of the vehicle [22],[23], defined as

$$J = \frac{d\ddot{p}}{dt} \quad (9)$$

where \ddot{p} is the vehicle longitudinal acceleration and t refers to time. Note that comfort and jerk act in contrast to each other. In order to achieve a satisfactory level of comfort, the absolute value of the jerk should be as small as possible. To measure this quantity, we use the following index:

- *Jerk signal Root Mean Square value:*

$$RMS_J = ||\tilde{J}||/\sqrt{N} \quad (10)$$

where \tilde{J} is the acquired (discrete-time) jerk of a vehicle.

- *Peak jerk signal:*

$$MAX_J = ||\tilde{J}||_{\infty}. \quad (11)$$

Figures 9 and 10 show the relationship between the averages of the root mean square values and the peak values of the jerk and spacing errors for both the Pareto optimal vehicles and “standard” vehicles. It can be seen that the same amount of jerk matches a lower spacing error for the Pareto optimal vehicle

and a higher spacing error for the “standard” vehicle. When the spacing errors in figure 9 are traced to figure 6, the required command input for the Pareto optimal vehicle is always lower than that of the “standard” vehicle. This demonstrates further that a Pareto optimal controller could give a better all around performance in terms of safety, comfort and fuel consumption.

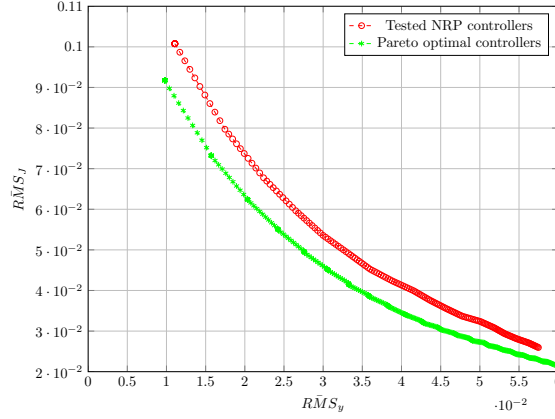


Fig. 9. Plot of average spacing errors and jerk

6 Conclusions

In spite of the benefits that passengers stand to gain from the use of ACCs, most passengers would rather not to use ACCs due to reliability and comfort concerns. Indeed, autonomous ACC policies that take all the necessary factors into account needed for the overall satisfaction of a customer are almost non-existent. This paper addresses this issue in two steps. In the first step, a systematic simulation procedure is developed for comparing different Adaptive Cruise Control (ACC) policies. This is needed to develop a proper understanding of how different ACC policies would react to different situations. In the second step, a multi-objective optimization technique, based on a Pareto efficiency criterion is proposed and tested. The optimal controller designed by means of this technique shows better

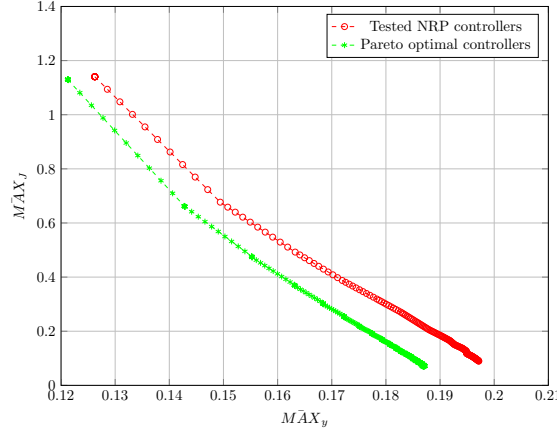


Fig. 10. Plot of peak values of spacing errors and jerk

results when compared with the “standard” ACC policies in terms of safety, fuel consumption and comfort. As a part of ongoing efforts to make ACCs more effective, future research activities will focus on extending the numerical simulations considered in this paper to curve situations where the radar is unable to sense the vehicle in front for a while and on developing a user-friendly performance ACC optimization toolbox.

References

1. L. Xiao and F. Gao. (2010). A Comprehensive Review of the development of Adaptive Cruise Control Systems. *Vehicle System Dynamics*, pages 1167–1192.
2. B. Howard.(2013). What is Adaptive Cruise Control, and how does it work? <http://www.extremetech.com/extreme/157172-what-is-adaptive-cruise-control-and-how-does-it-work>.
3. P. Shakouri, A. Ordys, and M. Askari. (2012.) Adaptive Cruise Control with stop & go function using the State-dependent Nonlinear Predictive control approach. *ISA Transactions* 51 Elsevier.
4. P. Shakouri and A. Ordys. (2014). Nonlinear Model Predictive Control approach in design of Adaptive Cruise Control with automated switching to cruise control. *Control Engineering Practice* 26, pages 160–177.

5. R. Rajamani. (2012). *Vehicle Dynamics and Control*. Mechanical Engineering Series Springer 2nd ed.
6. W. Schakel, B. Arem and B. Netten. (2010). Effects of Cooperative Adaptive Cruise Control on Traffic Flow Stability. *Proceedings of the 13th IEEE Annual Conference on Intelligent Transportation Systems*, pages 759–764.
7. S. Oncu, N. Wouw and H. Nijmeijer. (2011). Cooperative Adaptive Cruise Control: Tradeoffs between Control and Network Specifications. *Proceedings of the 14th International IEEE Conference on Intelligent Transportation Systems*, pages 2051–2056.
8. D. Swaroop. (1995). *String Stability of Interconnected Systems: An Application to Platooning in Automated Highway Systems*. PhD dissertation, Dept. Mechanical Eng., Univ. California Berkeley.
9. D. Yanakiev and I. Kanellakopoulos. (1995). Variable Time Headway for String Stability of Automated Heavy-Duty Vehicles. *Proceedings of the 34th IEEE Conference on Decision and Control*, pages 4077–4081.
10. D. Yanakiev and I. Kanellakopoulos. (1995). Variable Longitudinal Control of Heavy-Duty Vehicles for Automated Highway Systems. *Proceedings of the American Control Conference*, pages 3096–3100.
11. D. Yanakiev and I. Kanellakopoulos. (1998). Nonlinear Spacing Policies for Automated Heavy-Duty Vehicles. *IEEE Transactions on Vehicular Technology* volume 47, pages 1365–1377.
12. K. Santhanakrishnan and R. Rajamani. (2003). On Spacing Policies for Highway Vehicle Automation. *IEEE Transactions on Intelligent Transportation Systems* Volume 4, pages 198–204.
13. D. Swaroop, J. Hedrick, C. Chien and P Ioannou. (1994). A Comparison of Spacing and Headway Control Laws for Automatically Controlled Vehicles. *Vehicle System Dynamics: International Journal of Vehicle Mechanics and Mobility*, pages 597–625.
14. L. Chi-Ying and P. Huei. (1999). Optimal Adaptive Cruise Control with Guaranteed String Stability. *Vehicle System Dynamics* 31, pages 313–330.
15. D. Swaroop and R. Hundra. (1998) Intelligent Cruise Control System Design based on a Traffic Flow Specification. *Vehicle System Dynamics* volume 30, pages 319–344.
16. J. Zhou and H. Peng. (2004). Range Policy of Adaptive Cruise Control Vehicles for Improved Flow and String Stability. *Proceedings of the IEEE International Conference on Networking, Sensing and Control*, pages 595–600.

17. J. Zhao, M. Oya and A. Kamel. (2009). A Safety Spacing Policy and its Impact on Highway Traffic Flow. *Intelligent Vehicles Symposium*, pages 960–965.
18. J. Wang and R. Rajamani. (2004). Should Adaptive Cruise-Control Systems be designed to maintain a Constant Time Gap between Vehicles? *IEEE Transactions on Vehicular Technology volume 53*, pages 1480–1490.
19. J. Wang and R. Rajamani. (2002). Adaptive Cruise Control System Design and Its Impact on Highway Traffic Flow. *Proceedings of American Control Conference*, pages 3690–3695.
20. J. Zhou and H. Peng. (2005). Range Policy of Adaptive Cruise Control Vehicles for Improved Flow and String Stability. *IEEE Transactions on Intelligent Transportation Systems Volume 6*, pages 229–237.
21. B. Brownstein. (1980). Pareto Optimality, External Benefits and Public Goods: A Subjectivist Approach. *Journal of Libertarian Studies*, pages 93–106.
22. L. Luo, H. Li, P. Li and H. Wang. (2010). Model predictive control for adaptive cruise control with multi-objectives: comfort, fuel-economy, safety and car-following. *Journal of Zhejiang University SCIENCE*, pages 191–201.
23. J.J. Martinez and C. Canudas-de-Wit. (2007). A safe longitudinal control for adaptive cruise control and stop-and-go scenarios. *IEEE Transactions on control systems technology*, pages 246–258.